Design, Modeling and Closed Loop Control of a Complementary Clamp Piezoworm Stage

S. P. Salisbury, *Member, IEEE*, R. Ben Mrad, *Member, IEEE*, D. Waechter, *Member, IEEE*, and S. E. Prasad

***Abstract*— A novel complementary clamp piezoworm stage was developed to be integrated into a two-axis configuration for tracking profiles in different size regimes. It is based on novel clamp designs which permit complementary action using the same flexure frame in a compact arrangement. A novel direct connection to a commercial slide was used to eliminate backlash and the need for high precision alignment of a rod and slide. A model was developed and used to design the controller structure and choose thresholds for smooth operation. Complete assessment of the closed loop performance of a single axis and dual axis stage in different regimes was performed. The average positioning accuracy of the stage was ±20 nm. For tracking applications, the average error of the two-axis stage was 8 nm in the nanometer regime, 1.72 µm in the micrometer regime and 1.85 µm in the millimeter regime.**

Index Terms— Complementary, piezoworm, precision, stage, control

I. Introduction

MANY active areas of research such as genomics, proteomics and MEMS/NEMS manufacture [1-6] require a two-axis stage capable of nanometer accuracy while having a range of several millimeters. The stage may be required to perform point-to-point positioning or to track a profile. The typical approach to address both large range and high accuracy is to mount a high accuracy actuator, such as a piezoelectric flexure stage, to a large range actuator, such as a linear motor [2,4,5]. However, this is bulky and complex to control especially if extrapolated to two axes of motion. A different approach is to use a piezoworm-based (also called inchworm®) system which has two clamping piezostack actuators and an extender piezostack actuator mounted in a flexure frame. To traverse long distances, a sequence of clamp-extend-clamp steps is executed [6]. The piezoworm can also adjust its position within one step by keeping one clamp fixed and finely varying the extender piezostack to achieve nanometer accuracy. This paper investigates using a two-axis complementary-clamp-based piezoworm stage to track profiles in the nanometer, micrometer and millimeter regimes.

The complementary clamp piezoworm actuator concept was first described in [9]. The actuator's two clamps are mechanically designed to grip on the opposite extremes of a common clamp signal. The clamp which grips at zero voltage is termed the normally-clamped (NC) clamp, and the other clamp which grips on high voltage is termed the normally-unclamped (NU) clamp. This arrangement reduces the number of amplifiers from three to two for a significant cost savings. The first generation design was developed for satellite reflector distortion compensation but the design is not suitable for two-axis stage integration because of its size, clamp mounting arrangement and control structure.

The footprint of the two-axis stage must be minimized to facilitate its integration into more complex laboratory systems and this leads to a preferred parallel-kinematics arrangement of the two axes. Mass must be minimized as well since the lower axis must drive the mass of the second axis plus the payload. High force capacity designs in the literature [6,11,23] typically have an actuator moving through a guideway with thick walls which makes the design too heavy to be used in a parallel-kinematics configuration. The other prominent design in the literature [8,9,10] has a fixed actuator and translates a rod. The actuator is small and is more suitable for a parallel-kinematics arrangement except that the rod must be coupled to a slide in order to mount the payload. The interface of the slide to the rod must be carefully assembled so that there is no backlash at the coupling and that the slide and rod motion are in perfect alignment so that jamming will not occur. The design in this paper has a fixed actuator but acts on the slide directly without the need for a coupling mechanism which improves the ease of alignment and integration. The design also has a novel complementary clamp design which reduces the size of the actuator and permits it to be used in a parallel configuration.

A closed loop controller must be used for the best tracking performance. Controllers based on varying either the frequency or amplitude full steps [24,25] do not take

Manuscript received July 18, 2008. This work was supported by the Ontario Centres of Excellence, Sensor Technology Limited and the National Sciences and Engineering Research Council of Canada. Shaun Salisbury is with the Department of Mechanical and Industrial Engineering, University of Toronto, 5 King's College Rd, Toronto, ON M5S 3G8, Canada (e-mail: ssalisbu@mie.utoronto.ca).

Ridha Ben Mrad is with the Department of Mechanical and Industrial Engineering, University of Toronto, 5 King's College Rd, Toronto, ON M5S 3G8, Canada (phone: 416-946-0689; e-mail: rbenmrad@mie.utoronto.ca).

David F. Waechter is with Nerac, Inc., One Technology Drive, Tolland, CT, USA, 06084 (e-mail: dwaechter@nerac.com).

S. Eswar Prasad is with Sensor Technology Limited, PO Box 97, Collingwood, ON L9Y 3Z4 Canada (e-mail: eprasad@sensortech.ca)..

advantage of the high accuracy performance within one step. For the highest accuracy, a composite controller is used which has one sub-controller to manage the clamps (supervisory) and another sub-controller (regulatory) to control the extension piezostack [20,21,22]. The supervisory controller is rule-based which depends on the structure of the piezoworm. For tracking control, the actuator should be in control of the slide at all times so that the error is minimized. In [20,21], the stage position was coupled to only one clamp so if the required motion exceeded one step then the controller cannot influence the stage position until the supervisory controller completes the cycle of: switching clamps, repositioning the extender piezostack and then re-engaging the coupled clamp. The complementary clamp piezoworm stage design presented in this paper has a fixed center section and either clamp can engage the stage. Its controller resembles that of [21] but [21] required an additional position sensor feeding the supervisory controller the relative position of the clamps. The controller in this paper instead uses the extender piezostack voltage which does not require an additional sensor. Also, the controller in [21] would switch between coarse and fine positioning modes whereas the controller in this paper does not switch modes and is always capable of fine positioning.

A dynamic model was used to simulate the performance of the stage system in order to evaluate switching laws and tune the regulatory controller. It uses a lumped parameter approach to the system as in [21] and [26] but it includes an improved model for the clamp behavior accounting for the gap at the interface and the friction capacity as a function of clamp voltage. Previous models [21,26] had assumed instantaneous switching which is not physically possible and the improved model was able to assess the effect of finite clamp switching time on tracking performance.

This paper describes the design, modeling and control of a two-axis stage based on an improved complementary clamp piezoworm actuator. Novel designs for the clamps are presented which improve the control and permit the use of the piezoworm in a parallel-kinematics configuration. A clamp arrangement more suitable for tracking was chosen and a novel connection to a commercial slide is described which avoids the need of precise alignment and eliminates backlash. A simulation model is also described which captures clamp behavior and allows study of tracking performance. The prototype complementary clamp piezoworm stage with the improved clamp designs is described in Section 2. Then, in Section 3, the dynamic model with clamp behavior is detailed. The development of the closed loop controller and performance is detailed in Section 4. The two-axis stage and tracking results in different regimes are presented in Section 5. Conclusions are summarized in Section 6.

II. STAGE DESIGN

The objective is to design a stage to have a range of at least 50 mm, maximize speed, stiffness and thrust while minimizing

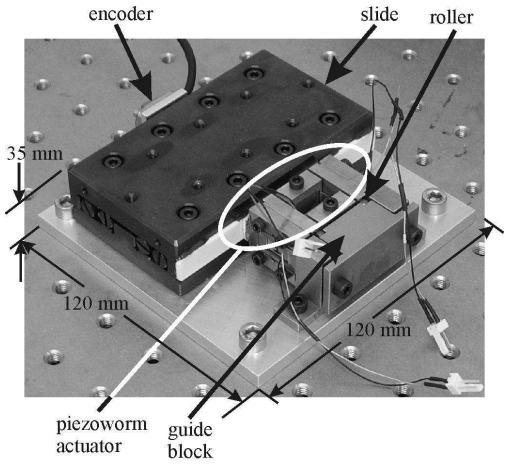

Fig. 1. Piezoworm stage prototype.

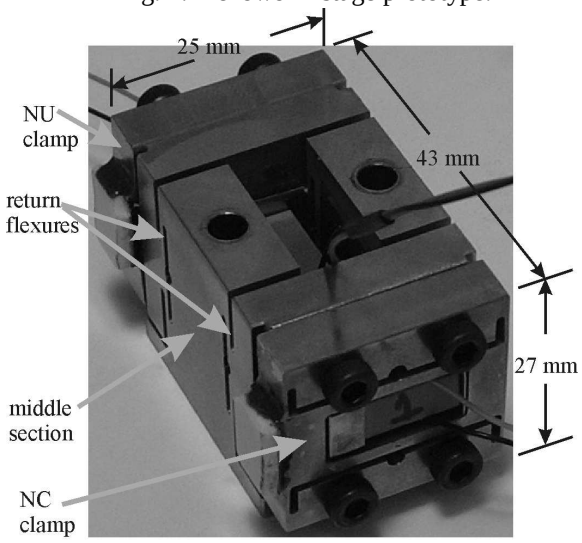

Fig 2. Piezoworm actuator.

the mass and size. Mass is critical for constructing a two-axis stage because the second axis is mounted on top of the first at 90° so the lower axis must be able to move the payload plus the mass of the upper axis. Other design goals are to minimize wear and cost.

The piezoworm stage prototype is shown in Fig. 1. The piezoworm actuator is mounted on a base plate and directly acts on a friction strip mounted on a crossed-roller slide. An encoder is mounted on the other side of the slide which is used for position measurement and has a resolution of 10 nm. Unlike most other designs [6, 10, 11], this piezoworm actuator pushes on only one side of the slide. This reduces the force transfer to the slide but permits a commercially available slide to be integrated into the design which reduces the cost. Jamming is also prevented with this arrangement since the piezoworm can adjust for the deviations of the slide as it travels through its range. With the direct coupling, backlash is not an issue.

The piezoworm actuator is an improved version of the complementary clamp actuator developed in [9] and is shown in Fig. 2. The piezoworm design in [9] is not suitable for two-axis stage integration because of its size and clamp mounting

arrangement. The NC clamp was fixed to the structure and all the motion was performed by the NU clamp. This work presents an improved complementary clamp piezoworm stage design which has the clamps connected to a middle section via extension flexures. This allows both clamps to be mobile which will permit control of the slide no matter which clamp is contacting the slide. The extension flexures are used as return springs to ensure that the piezostack does not experience damaging shear or tensile loads. Machined flexures are used instead of springs that were in [9] to be able to achieve sufficient stiffness to ensure the frame resonant frequency is above the excitation frequency. The maximum operating frequency of the amplifier driving the piezoceramics is 800 Hz which is determined by its peak current of 1 A at 200 V.

A. Clamp Design

The clamp configurations are shown in Fig. 3. Both clamps use the same piezostack made of Navy Type II PZT (Sensor Technology BM500) having a free expansion of 12 µm and a stiffness of 60 N/µm. These piezostacks were chosen because they offer good free expansion and high stiffness in a small package size. The expansion dictates the stroke of the clamps and the larger the stroke the more accommodation for slide variation. Ceramic strips are glued to the friction surfaces of the clamps and to the slide to reduce wear.

Flexures are used to preload and protect the piezostacks. The clamps have almost identical flexure frames with only the bottom hole being different. The NC clamp has a tapped hole for a set screw, whereas the NU clamp has a through hole to permit adjustment of a set screw on the tab from the extension frame to preload the piezostack. The clamp flexure frame is bolted to the extension frame via four screws through the mounting holes. The orientation of the tab that extends from the extension frame through the clamp frame determines whether the clamp acts as a NU or NC clamp. The NU clamp has the tab oriented such that the expansion of the piezostack will cause the clamping surface to move toward the slide and maximum clamping force is achieved when the piezostack is fully energized. The NC clamp has the tab on the side closest to the clamping surface. The extension of the piezostack causes the clamping surface to move away from the slide eventually creating a gap when the piezostack is fully energized.

Using a common flexure frame configuration has several advantages. The mass of the NU clamp and NC are identical so that we can expect their dynamic behaviour also to be identical. Additionally, several clamp frames can be fabricated simultaneously using wire electrical discharge machining (EDM). This reduces cost and if a clamp is damaged, it could be exchanged for a new clamp instead of scrapping the entire piezoworm.

III. Dynamic Model

A simulation model was developed to assess the controller structure and develop the controller parameters for the stage. The lumped parameter model is shown in Fig. 4 and the equations of motion are given in (1) to (3). Each clamp is represented as a mass (m_{NU}, m_{NC}) coupled to a rigid centre section via a spring (k_{NU}, k_{NC}) and damper (c_{NU}, c_{NC}) which represent the return flexures. The slide and any payload are lumped into one mass, m_S, and the friction forces, F_{NU} and F_{NC}, are the interface between the clamps and the slide. A linear model for the extension piezostack was adopted based on the IEEE piezoelectric linear model [13]. F_P is the force from the extender piezostack and is determined by (4) given k_p as the piezo stiffness, L_o its free expansion at V_{MAX} and V_{EXT} is the applied voltage.

$$m_{NU}\ddot{x}_{NU} = F_P - c_{NU}\dot{x}_{NU} - k_{NU}x_{NU} - F_{NU} \quad (1)$$

$$m_{NC}\ddot{x}_{NC} = -F_P - c_{NC}\dot{x}_{NC} - k_{NC}x_{NC} - F_{NC} \quad (2)$$

$$m_S\ddot{x}_S = F_{NU} + F_{NC} + F_d \quad (3)$$

$$F_P = \frac{k_p L_o}{V_{MAX}} V_{EXT} - k_p(x_{NU} - x_{NC}) \quad (4)$$

To determine the friction force between the clamps and the slide, a method similar to that in [21] is used based on the stiction plus Coulomb friction model and is given by (5a) and (5b). This can be summarized as follows. If the difference in velocity between a clamp and the slide is within a threshold ((6a) and (6b)), then the friction force is proportional to the applied load, $F_{applied}$. The clamp and slide may be considered as stuck together, acting as a single mass, provided that the friction between them is below the maximum (F_{NUmax}, F_{NCmax}). If the applied load exceeds the maximum friction force the clamp can provide or the relative velocity is above the threshold, then the clamp friction force is equal to the maximum clamp friction force. A small threshold velocity is used in the simulation instead of zero to aid simulation convergence.

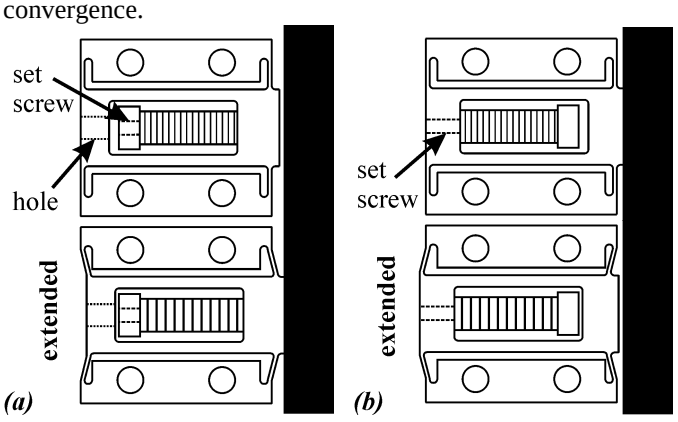

Fig. 3. a) NU clamp, b) NC clamp.

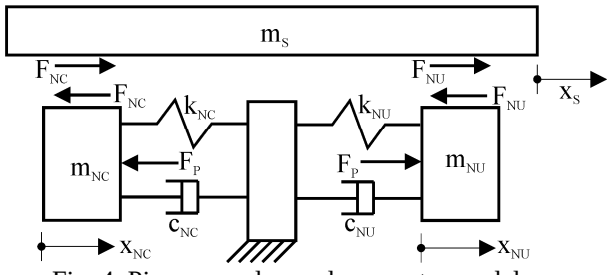

Fig. 4. Piezoworm lumped parameter model.

An improved model is used to determine the maximum friction force (F_{NUmax}, F_{NCmax}) of each clamp from the common clamp voltage, V_C. In [21, 26] the clamps were assumed to switch instantly from clamped to unclamped and the gap between the clamp and slide was ignored. While it was shown in [9] that the clamp force follows closely the applied voltage, limits on the amplifier current restrict the rate at which the voltage can be changed. The finite switching time and the gap can significantly affect the tracking performance so they must be accounted for. The masses involved in clamp switching are small compared to the stiffnesses so their dynamic effects can be ignored. The clamp behavior is based on the models shown in Fig. 5 and given by (7a) and (7b). The threshold voltage (V_{NUT}, V_{NCT}) represents the gap between the clamping surfaces and the slide which exists in practical designs to allow for misalignment. The slope of the curve (r_{NU}, r_{NC}) and the threshold can be calculated from the physical characteristics of the clamps as in [9] or could be experimentally determined.

$$F_{NU} = \begin{cases} \text{sgn}(\dot{x}_{relNU}) F_{NU\max} & |\dot{x}_{relNU}| \geq \dot{x}_0 \\ sat\left(\dfrac{F_{applied}}{F_{NU\max}}\right) F_{NU\max} & |\dot{x}_{relNU}| < \dot{x}_0 \end{cases} \quad (5a)$$

$$F_{NC} = \begin{cases} \text{sgn}(\dot{x}_{relNC}) F_{NC\max} & |\dot{x}_{relNC}| \geq \dot{x}_0 \\ sat\left(\dfrac{F_{applied}}{F_{NC\max}}\right) F_{NC\max} & |\dot{x}_{relNC}| < \dot{x}_0 \end{cases} \quad (5b)$$

$$\dot{x}_{relNU} = \dot{x}_{NU} - \dot{x}_S \quad (6a)$$

$$\dot{x}_{relNC} = \dot{x}_{NC} - \dot{x}_S \quad (6b)$$

$$F_{NU\max} = \begin{cases} 0 & for \quad V_C < V_{NUT} \\ r_{NU}(V_C - V_{NUT}) & for \quad V_C \geq V_{NUT} \end{cases} \quad (7a)$$

$$F_{NC\max} = \begin{cases} r_{NC}(V_C - V_{NCT}) & for \quad V_C < V_{NCT} \\ 0 & for \quad V_C \geq V_{NCT} \end{cases} \quad (7b)$$

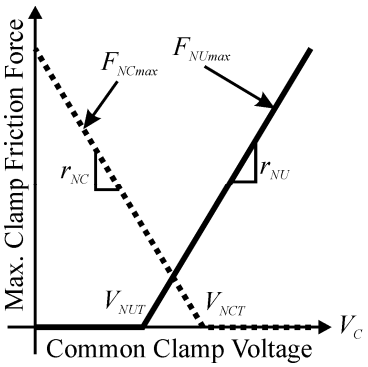

Fig. 5. Clamp friction force capacity vs. voltage characteristic.

IV. Closed Loop Control and Performance

Closed loop control of the piezoworm is required to realize accurate positioning and tracking. The controller must address the limitation on the extender voltage which limits its stroke. Also, the number of sensors required should be minimized to limit cost. A composite controller is employed for this system (see Fig. 6) separated into a supervisory and a regulatory sub-controller. The system uses only one sensor which is the position of the slide, x_S.

A sampling frequency of 10 kHz was chosen because it gave sufficient time to complete all the control tasks in one control cycle and it also made favorable plant pole locations when the plant transfer function was discretized.

The supervisory sub-controller has two tasks; manage the clamp switching and select the appropriate control law for the regulatory controller. The previous extension signal, u_{EXT}, from the regulatory controller and the current error signal, e, are used to determine if clamp switching is needed. If the extension signal is at its limit and the current error signal indicates the new extension signal will be outside its limit then a clamp switch is performed. This is summarized in the control law shown in (8) where the extension signal upper limit is u_{UL} and the lower limit is u_{LL}. The clamp signal, u_C, is used to account for which clamp is engaged. If u_C is zero then the NC clamp is engaged, and if it is ten then the NU clamp is engaged. Use of the extender signal, u_{EXT}, is in contrast to the switching law proposed in [21] which used the relative displacement of the two clamps measured by an additional sensor. This is more costly and the relative displacement will vary depending on the load on the piezostacks which makes selecting the switching limits challenging.

$$\begin{aligned} &\left(u_{EXT} = u_{UL} \quad AND \quad e \times (-1)^{u_C} > 0\right) \\ &OR \quad \left(u_{EXT} = u_{LL} \quad AND \quad e \times (-1)^{u_C} < 0\right) \end{aligned} \quad (8)$$

Indeed, the switching limits are the critical aspect of the supervisory controller. Noise on the error signal and the glitching [6] that occurs when the clamps are switched can cause the supervisory controller to oscillate between switch states especially during tracking when the error signal is small and perturbations can alter the sign of the error signal. This is accommodated by having hysteretic limits as was suggested in [22]. Initially, the limits are set inside the range of the extension signal but when the switch condition is met the limit involved is increased. The limit is maintained at this value until the extender signal drops below a threshold. For the piezostage, the maximum limits for the piezostack signal are zero and ten volts and the initial limits were determined through simulation studies to be set at two and eight volts. This was to give sufficient room for the regulatory controller to compensate for glitching.

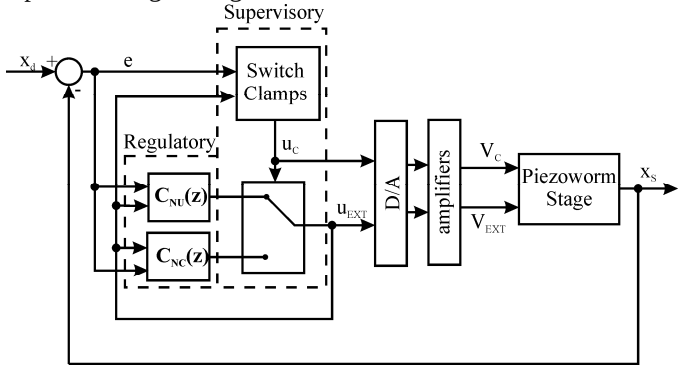

Fig. 6. Controller block diagram.

The supervisory controller also determines which regulatory controller sends the output signal to the extender piezostack based on which clamp is gripping the slide. Both regulatory controllers receive the error and previous output signals so that no initialization is required when switching from one regulatory controller to the other. Previous controllers [20, 21] used mode switching which can be problematic for tracking since the profile may require constant alternating between the two modes and the regulatory controller may need to be initialized each time.

A. Regulatory Controller

The regulatory controller determines the extender signal for tracking control. The piezoworm was designed to be symmetrical so that the control law developed for one clamp will be the same for the other with a change in sign to account for the opposite actuation direction. The slide moves in the positive direction when the piezostack elongates with the NU clamp engaged as shown in Fig. 4. The controller needs to be designed to provide high accuracy, fast response but is subject to the extender piezostack voltage limitation. Improved tracking accuracy may be achieved if hysteresis compensation is used however the methods developed in the literature [27, 28] require direct measurement and storage of the extender piezostack displacement. The controller in this work measures the slide position only. Hysteresis compensation was not pursued.

Assuming the slide is rigidly connected to the NU clamp, a transfer function was developed by combining (1) to (4) using the parameters in Table I. The transfer function was then converted to its discrete-time equivalent using MATLAB [15] zeroth-order-hold approximation (i.e. intersample behavior assumed constant) at a sample frequency of 10 kHz. The resulting plant equation is shown in (9). Due to symmetry, the transfer function when the NC clamp is engaged is assumed to be the negative of (9).

$$G(z)=\frac{X_S(z)}{V_{EXT}(z)}=\frac{0.282z^{-1}+0.363z^{-2}+0.315z^{-3}+0.139z^{-4}}{1-0.407z^{-1}+0.436z^{-2}+0.102z^{-3}+0.544z^{-4}} \quad (9)$$

TABLE I - SIMULATION PARAMETERS

Parameter	Value
m_{NU}, m_{NC}	45 g
k_{NU}, k_{NC}	37 N/µm
c_{NU}, c_{NC}	258 N•s/m
r_{NU}	0.0533 N/V
V_{NUT}	20 V
m_S	685 g
k_P	38 N/µm
L_o	19.5 µm
r_{NC}	-0.0533 N/V
V_{NCT}	180 V
V_{MAX}	200 V

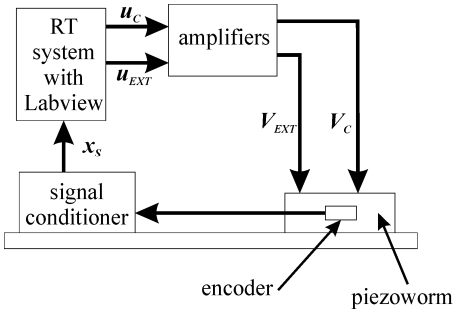

Fig. 7. Prototype experimental setup.

A closed loop controller was developed based on (9) by direct design using the z-plane root locus approach in MATLAB. The open-loop system is type zero which means that the closed-loop system would have a finite steady-state error for a step input. A pole was added on the unit circle for an integrator to eliminate the steady-state error. An additional pole at -0.1643 and zeros at 0.736 and 0.7561 were selected to improve the transient performance. The final controller for the NU clamp gripping the slide is given in (10) with K=3.132. The controller for when the NC clamp is active, $C_{NC}(z)$, is the negative of (10).

$$C_{NU}(z)=K\frac{1-1.519z^{-1}+0.577z^{-2}}{1-0.8357z^{-1}-0.1643z^{-2}} \quad (10)$$

The prototype was subjected to several tests to assess its performance and compare it to the dynamic model implemented in Simulink [15]. The test setup is shown in Fig. 7. The piezoworm stage was mounted to a breadboard table with the NC clamp on the left side viewed from the perspective of Fig. 7. The encoder mounted to the slide (MicroE Systems Mercury 3500 with a resolution of 10 nm) was used to measure the position, x_S. A signal conditioning module changes the encoder signal into a standard signal that can be read by Labview RT [16] running on a PC. The controller was implemented in the PC and supplied the control signals, u_C and u_{EXT}, which are from 0 to 10 V. The amplifiers, two DSM VF-500 [17], have a gain of 20 to boost the signal to a maximum of 200 V. The common clamp voltage, V_C, splits to provide the signal to each clamp, while the extender signal, V_{EXT}, controls the extender piezostack.

First, the stage performance and open loop model $G(z)$ was verified experimentally in a similar manner to the procedure presented in [20]. The stage had a top speed of 8.5 mm/s which is faster than the commercially-available EXFO inchworm (1.5 mm/s) [29] but slower than the PI ultrasonic stage (400 mm/s) [30]. The thrust force of 6 N and a load carrying capacity of 17 kg are similar to EXFO but is much larger than the PI stage which has a load capacity of 5 kg [30].

Next, a closed-loop step command of 1 µm was issued which tests only the regulatory controller. The results in Fig. 8 show an excellent response time of about 10 ms with no overshoot and a steady-state error of ±10 nm, which is due to the resolution of the encoder. The model and prototype performance show good correlation. The oscillation in the experimental results is from the controller combined with the

hysteresis effect. Sinusoidal tests of displacements smaller than one full step showed a closed-loop bandwidth of 75 Hz.

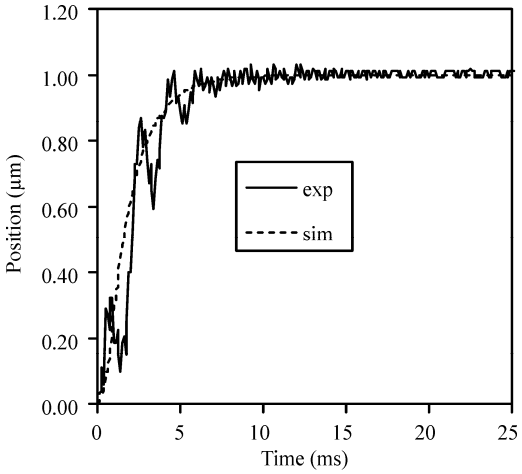

Fig. 8. Position vs. time for closed-loop step test.

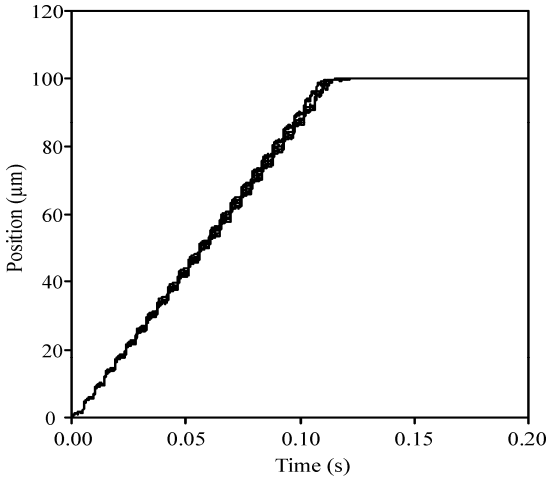

Fig. 9. Five responses to a step command of 100 µm.

The control system was tested using a command of 100 µm. Both the supervisory and the regulatory controller are active since the command is greater than one step of the piezoworm. This was repeated five times to observe the repeatability. Fig. 9 shows that both sub-controllers functioned well and the position was repeatable to ±10 nm. The PI ultrasonic stage can only achieve a repeatability of ±300 nm [30].

The next test involves tracking a sine wave which is more demanding than the step commands because the glitching effect is more prominent and there are errors due to the finite time to switch clamps. Fig. 10a shows the position and tracking error of the control system for a 1 Hz, 20 µm sine wave. The spikes in the error are due to glitching and clamp switching and can cause errors of ±500 nm whereas the errors at other times are between ±200 nm and even less if the error due to the phase difference is accounted for. The duration of the spikes is about 10 ms which corresponds to the response time of the regulatory controller shown earlier in Fig. 8. The simulation results in Fig. 10b show the error due to clamp switching alone and even without glitching the errors can be as much as 375 nm. This is important since it puts a limit on the achievable tracking accuracy of the piezoworm stage. Higher power amplifiers would allow quicker change of the signal and should reduce the finite switch time effect.

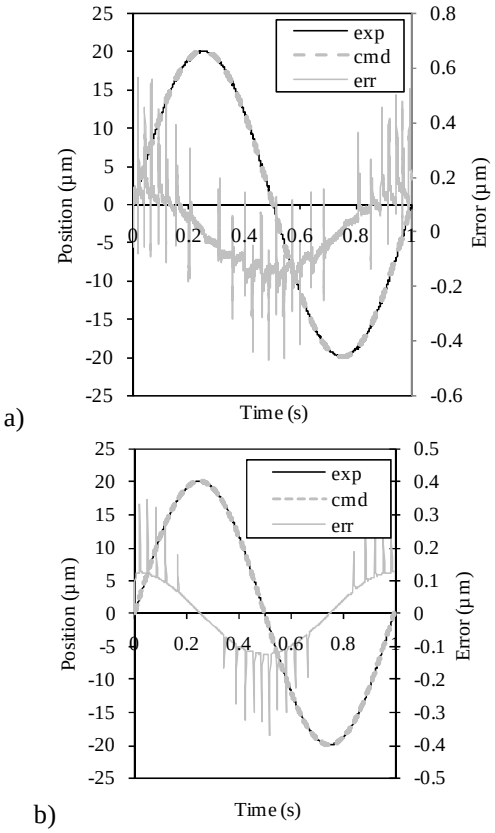

Fig. 10. (a) Experimental results for tracking a 1 Hz, 20 µm sine wave. (b) Simulation results for tracking a 1 Hz, 20 µm sine wave.

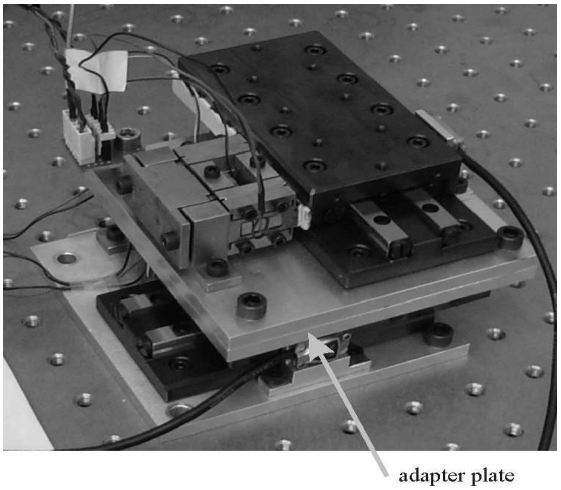

Fig. 11. Two-axis stage prototype.

V. Two-Axis Stage

A second prototype was constructed and mounted to the slide of the first via an adapter plate as shown in Fig. 11. The second axis was driven with an identical controller through its own amplifiers.

Several tracking tests were performed on the two-axis stage covering different regimes. The first was in the nanometer regime and the commanded profile and results are shown in Fig. 12a. The tracking error was calculated based on the root-mean-squared (RMS) formula in (11) and is shown Fig. 12b. Most of the error is due to noise in the encoders which is about ±20 nm. It is due to environmental conditions including building vibration and variations in temperature and pressure of the air. If a more controlled environment were implemented then the low frequency noise could be reduced. In spite of the noise, the two-axis stage shows good tracking in this regime and the average error is 8 nm.

The next test was in the micrometer regime tracing out the same shape but at a larger scale as shown in Fig. 13a with error in Fig. 13b. The error contains the effect of glitching, finite clamp switch time and cross-coupling between the axes. The average tracking error was 1.72 µm.

Finally, the millimeter regime was explored using the shape scaled by two orders of magnitude. The profile is shown in Fig. 14a with the error in Fig. 14b. The average error in this regime was 1.85 µm – a slight increase from the micrometre regime. The error is composed of the same effects also in the micrometer regime.

$$tracking\ error = \sqrt{x_{error}^{\ 2} + y_{error}^{\ 2}} \tag{11}$$

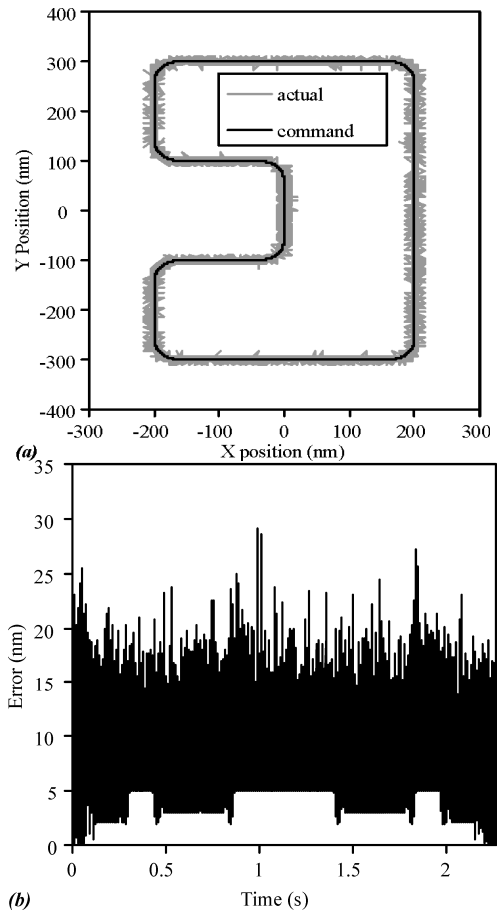

Fig. 12. (a)Tracking profile in nanometer regime. (b)Tracking RMS error in nanometer regime.

VI. Conclusions

A novel piezoworm stage was developed which was designed specifically as a stage. It is based on novel clamp designs which permit complementary action using the same flexure frame in a compact arrangement. A novel direct connection to a commercial slide was used to eliminate backlash and the need for high precision alignment of a rod and slide.

A closed loop tracking control was described which is based on a supervisor which manages clamping and a regulator which precisely controls the extension actuator. For a 1 µm step command, the closed loop system has no overshoot, a settling time of 10 ms and a steady state error in the noise floor of the encoder. Similar positioning accuracy was demonstrated for a command of 100 µm. The accuracy when tracking sinusoidal inputs larger than one step is dependent on the glitching when the clamps switch and also the finite time required to switch the clamps.

A dynamic model used for simulation was presented which included a model for the clamp behavior. This model showed that the tracking performance of the piezoworm for sinusoids is also dependent on the finite time it takes to switch clamps. Future tracking improvements could be realized by higher power amplifiers.

The novel stage was integrated into a two-axis positioning system and several profiles were tested to demonstrate the stage's ability to cover the different regimes of the motion. In the nanometer regime, the error is dominated by the noise in the encoder signal. The errors in the other regimes were dominated by glitching when the clamps switch. The stage is capable of high accuracy, point-to-point positioning over a large range which is useful for a wide range of applications. High accuracy tracking is possible if the profile does not cause the clamps to switch. The stage could track an array of nanometer-sized features and create micrometer- and millimeter-sized features on the same device.

Future work will include the investigation of using hysteresis compensation or charge amplifiers to improve the tracking performance.

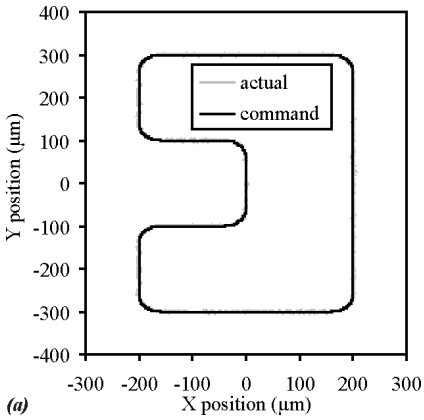

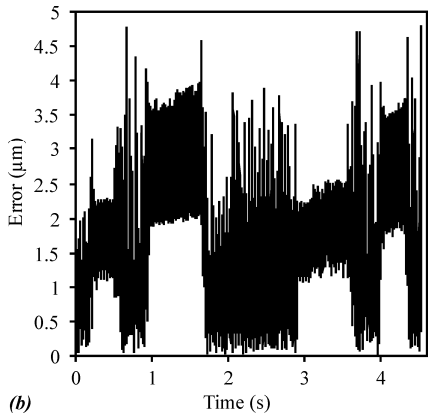

Fig. 13. (a)Tracking profile in micrometer regime. (b) Tracking RMS error in micrometer regime.

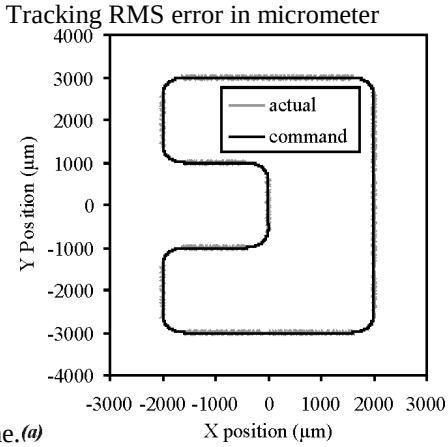

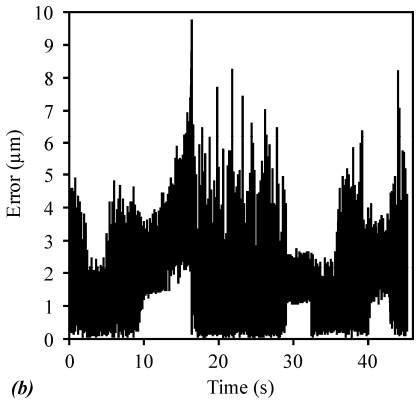

Fig. 14. (a) Tracking profile in millimeter regime. (b) Tracking RMS error in millimeter regime.

REFERENCES

[1] Y. Okazaki, "Precision Positioning Control Apparatus and Precision Positioning Control Method," US Patent 5 801 939, Sep. 1, 1998.

[2] W. Yao and M. Tomizuka, "Robust Controller Design for a Dual-Stage Positioning System," Proc. of International Conference on Industrial Electronics, Control, and Instrumentation, vol. 1, 1993, pp. 62-66.

[3] K. Tsai and J. Yen, "Servo System Design of a High-Resolution Piezo-Driven Fine Stage for Step-and Repeat Microlithography Systems," Proc. of Annual Conference of Industrial Electronics Society, vol. 1, 1999, pp. 11-16.

[4] S. Kwon, W. Chang and Y. Youm, "Robust and Time-Optimal Control Strategy for Coarse/Fine Dual-Stage Manipulators," Proc. of IEEE International Conference on Robotics and Automation, vol. 4, Apr. 2000, pp. 4051-4056.

[5] S. Kwon, W. Chang and Y. Youm, "On the Coarse/Fine Dual-Stage Manipulators with Robust Perturbation Compensator," Proc. of IEEE International Conference on Robotics and Automation, vol. 1, May 2001, pp. 121-126.

[6] B. Zhang and Z. Zhu, "Developing a Linear Piezomotor with Nanometer Resolution and High Stiffness," IEEE/ASME Transactions on Mechatronics, vol. 2, no. 1, Mar. 1997, pp. 22-29.

[7] M. Schena, "Microarray Analysis," John Wiley & Sons, New Jersey, 2003.

[8] D. Newton, E. Garcia and G. Horner, "A Linear piezoelectric Motor," Smart Materials and Structures, vol. 7, no. 3, 1998, pp. 295-304.

[9] S. Salisbury, D. F. Waechter, R. Ben Mrad, S. E. Prasad, R. G. Blacow, and B. Yan, "Design considerations for complementary inchworm actuators," IEEE/ASME Trans. on Mechatronics, vol. 11, no. 3, June 2006, pp. 265-272.

[10] W. May Jr., "Piezoelectric Electromechanical Translation Apparatus," US Patent 3 902 084, Aug. 26, 1975.

[11] P. Tenzer and R. Ben Mrad, "A systematic procedure for the design of piezoelectric piezoworm precision positioners," IEEE/ASME Transactions on Mechatronics, vol. 9, no. 2, June 2004, pp. 427-435.

[12] ANSYS, Version 9.0, Ansys Inc.

[13] IEEE Standard on Piezoelectricity, ANSI/IEEE Standard 176-1987.

[14] H. Khalil, Nonlinear Systems, New Jersey: Prentice-Hall, 2002.

[15] MATLAB, Version 6.5 Release 13, The MathWorks, Inc.

[16] LABVIEW Real-Time, Version 8.20, National Instruments Corp.

[17] "VF-500: Linear Piezo Amplifier", Dynamic Structures and Materials LLC, [Online document], [2005 January 10] Available at http://www.dynamic-structures.com.

[18] "FAQ," Burleigh, [Online document], [2002 July 17] Available at http://www.burleigh.com

[19] R. Ben Mrad and H. Hu, "Dynamic Modeling of Hysteresis in Piezoceramics," Proc. of IEEE/ASME International Conference on Advanced Intelligent Mechatronics, vol. 1, Jul. 2001, pp. 510-515.

[20] S. Salisbury, D. F. Waechter, R. Ben Mrad, S. E. Prasad, R. G. Blacow, and B. Yan, "Closed loop control of complementary clamp piezoworm actuator," IEEE/ASME Transactions on Mechatronics, Vol. 12, no. 6, Dec. 2007 pp. 590-598.

[21] R. Ben Mrad, A. Abhari and J. Zu, "A control methodology for an inchworm piezomotor," Mechanical Systems and Signal Processing, vol. 17, no. 2, 2003, pp. 457-471.

[22] C. Moon, S. Lee and J. Chung, "A new fast inchworm type actuator with the robust I/Q heterodyne interferometer feedback," Mechatronics, vol. 16, no. 2, Mar. 2006, pp. 105-110.

[23] J. Ni and Z. Zhu, "Design of a linear piezomotor with ultra-high stiffness and nanoprecision," IEEE/ASME Transactions on Mechatronics, vol. 5, no. 4, December 2000, pp. 441-443.

[24] E. Shamoto and T. Moriwaki, "Development of a walking drive ultraprecision positioner," Precision Engineering, vol. 20, no. 2, Mar. 1997, pp. 85-92.

[25] M. Versteyhe, D. Reynaerts and H. Van Brussel, "Hybrid force-position control of clamping with a piezo-stepper," IEEE Control Systems Magazine, vol. 19, no. 2, 1999, pp. 31-39.

[26] T. Galante, J. Frank, J. Bernard, W. Chen, G. Lesieutre, and G. Koopmann, "Design, Modeling, and Performance of a High Force Piezoelectric Piezoworm Motor," SPIE Proc. Smart Structures and Integrated Systems, vol. 3329, 1998, pp. 756-767.

[27] R. Ben Mrad and H. Hu, "Dynamic Modeling of Hysteresis in Piezoceramics," Proc. of IEEE/ASME International Conference on Advanced Intelligent Mechatronics, vol. 1, Jul. 2001, pp. 510-515.

[28] P. Ge and M. Jouaneh, "Modeling hysteresis in piezoceramic actuators," Prec. Eng., vol. 17, July 1995, pp. 211-221.

[29] "FAQ," Burleigh, [Online document], [2002 July 17] Available at http://www.burleigh.com.

[30] "M-665," Physik Instrumente GmbH & Co. [Online document], [2008 October 2] Available at http://www.physikinstrumente.com.